Isolating the Effect of Torsional Defects on Mobility and Band Gap in Conjugated Polymers

Seth B. Darling†

Center for Nanoscale Materials, Argonne National Laboratory, 9700 South Cass Avenue, Argonne, Illinois 60439

Received: February 29, 2008; Revised Manuscript Received: May 12, 2008

Conjugated polymers represent a promising class of organic semiconductors with potential applications in a variety of molecular devices. Poly(3-alkylthiophene)s, in particular, are garnering interest due to their large charge carrier mobility and band gap in the visible region of the spectrum. Defects play a pivotal role in determining the performance of polymer electronics, and yet the function of specific types of defects is still largely unknown. Density functional theory calculations of alkyl-substituted oligothiophenes are used to isolate the effect of static inter-ring torsion defects on key parameters such as electronic coupling between rings and band gap. Results have potential implications both for the fundamental understanding of intramolecular charge transport and for improving processing in organic devices.

Conjugated polymers have received increasing attention in recent years both for their potential application in organic electronics and optoelectronics and for the insight they can provide in fundamental issues connecting electronic structure and molecular geometry.[1–5] In large part, industrial interest draws from the fact that π-conjugated organic materials are considerably easier to process than traditional inorganic semiconductors. All layers can be fabricated near room temperature, largely with solution processing. Additional advantages include lower cost, lower weight, and mechanical flexibility. For the majority of likely applications, parameters such as charge carrier mobility and band gap play critical roles influencing the device performance. Charge carriers are either injected into the polymer, in the case of light emitting diodes (LEDs) or field effect transistors (FETs), or created within the polymer itself by optical excitation and charge separation in photovoltaic (PV) systems. In LEDs, high mobility improves performance by reducing space charging and minimizing quenching; in PVs, it minimizes electron−hole recombination; in FETs, it facilitates high-frequency operation.

Polythiophenes and poly(3-alkylthiophene)s, in particular, are perhaps the most prevalent class of conjugated organic semiconductors.[1,2,6–8] For a given polymer, the mobility in, e.g., a FET device can vary by many orders of magnitude depending for the most part on processing rather than constituent material. For example, FETs constructed with polythiophene have exhibited hole mobilities on the order of 10^{-5} cm^2 V^{-1} s^{-1},[9] whereas those fabricated using regioregular poly(3-hexylthiophene) (P3HT, Figure 1) have mobilities as high as 0.1 cm^2 V^{-1} s^{-1}.[10,11] Traps located just below the polymer's lowest unoccupied molecular orbital (LUMO) generally lead to lower mobilities for electrons compared to holes, though recent theoretical and experimental work has shown that ambipolar transport is possible when the environment is rationally designed.[12] Because mobility is actually a measure of the cumulative contribution of innumerable material parameters, extensive effort has been directed at identifying the role of various internal and external factors. Molecular weight, annealing condition, grain size, polarization, electric field, light exposure, and interface material have all been investigated for their impact on hole mobility.[6,13–19] In particular, molecular weight and annealing, which in turn can impact grain size, affect the ordering of the polymer chains, and it is generally accepted that molecular disorder plays an important role in limiting the transport of charge carriers both along chains and between chains. Charge transport in organic semiconductors has been recently reviewed,[20,21] with the summary finding that description of mobility is surprisingly complex in this class of materials, with both electron−electron and electron−phonon coupling playing significant roles.[22]

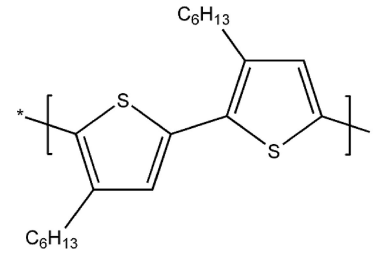

Figure 1. Regioregular P3HT chemical structure.

Despite all of this research, the role of particular molecular defects, which underlie much of the processing-mobility connection, remains largely unknown.[23,24] On the basis of experimental data on devices comparing, for example, as-prepared with annealed polymer films, it is believed that defects negatively affect performance. Most studies invoke direct current detection methods to probe bulk properties, which blur the components contributing to the overall mobility; generally, these approaches identify the most limiting kinetic process-typically migration between grains. In spite of the significant implications from both technological and fundamental scientific perspectives, the relative influence of specific types of defects is not clear. Much of this mystery stems from the fact that it is virtually impossible to decipher the role of individual defects experimentally. Recently, it has been shown that low-temperature STM can resolve individual torsional defects in isolated oligothiophene chains,[25] but experimentally connecting defect structure to electronic properties remains a challenge. Although crystal ordering driven by π-stacking of neighboring polymer chains[26]

† E-mail: darling@anl.gov.

10.1021/jp8017919 CCC: $40.75
Published on Web 07/03/2008

is an important factor in device performance, characterizing intramolecular mobility is a critical step toward decoding the inscrutability of defect roles, especially as device dimensions continue to approach molecular length scales. Important insight can be derived from coupling calculations with experiments.

Modeling polymeric semiconductors is challenging because periodic boundary conditions, often applied to polymers, are not especially useful in studies of isolated molecular defects. A corollary is that high level quantum chemical methods and large basis sets are too computationally expensive because many atoms ought to be included when periodicity cannot be exploited. To avoid lower-level theories that overlook subtle phenomena, a common approach is to use small molecular models that capture the essential behavior of the full polymeric system. Specifically, 2,2′-bonded oligothiophenes ($n \leq 8$) have been the focus of several electronic structure studies.[27–30] Given the flexibility of the polymer backbone inter-ring and intra-ring dihedral angles, a number of calculations have focused on torsional and ring disorder.[31–37] This body of work has almost exclusively simulated the comparatively small molecule bithiophene. In general, the alkyl side chains in polymers such as P3HT, which play important roles in solubility and intermolecular packing, are deemed unimportant from an electronic perspective and are therefore not included in most calculations. It is reported that density functional theory (DFT) is a reliable method for obtaining optimized geometries, electronic structure, frontier molecular orbital energies, and vibrational dynamics in this model system; there are, however, some reservations of the quantitative accuracy of DFT methods in modeling the torsional potential.[36]

Although the overall relative changes to the molecular energy during torsion are somewhat problematic, the work presented in this paper suggests that the relative changes to the frontier orbitals such as the highest occupied molecular orbital (HOMO) and LUMO are well-behaved and reasonably accurate. Earlier modeling has suggested that torsional disorder, i.e., nonplanar backbone structures, leads to a breaking of the MO delocalization and consequently hinders charge transport.[32] The theoretical construction used in this work models the polymer as a one-dimensional string of distinct monomers, the so-called tight binding approximation,[38] with no correlation between neighboring torsion angles. (This latter assumption can be reliably applied to isolated polymer chains but will have less relevance to solid state devices where interchain interactions produce ordered domains.) The figure of merit in this case is the electronic coupling, or the charge transfer integral (CTI), between neighboring thiophene rings:

$$|\mathrm{CTI}| = \frac{1}{2}\sqrt{(E_{\mathrm{HOMO-1,full}} - E_{\mathrm{HOMO,full}})^2 - (E_{\mathrm{HOMO,1}} - E_{\mathrm{HOMO,2}})^2} \quad (1)$$

where $E_{\mathrm{HOMO\text{-}1,full}}$ and $E_{\mathrm{HOMO,full}}$ are the energies of the two highest occupied molecular orbitals in the full molecular model and $E_{\mathrm{HOMO,1}}$ and $E_{\mathrm{HOMO,2}}$ are the HOMO energies in the two units at infinite separation. The approach used in the work presented here differs from a rigorous monomeric approximation in that fully planar sections of polymer are treated collectively as units (a reasonable methodology given the strong delocalization of the frontier molecular orbitals in planar chains). The current study suggests that, when a more inclusive molecular model is employed, the negative impact of torsional rotation is lessened in some cases. This work has potential ramifications both for interpreting intramolecular charge transport and for semiconductor device applications.

Because high level quantum chemical methods are too cumbersome to explicitly model lengthy oligothiophenes with alkyl side chains, DFT (B3LYP functional) was selected for this study (as implemented in Gaussian 03[39]). The B3LYP functional is generally reliable for predictions of geometries; energy calculations require further scrutiny. To determine the accuracy of this approach for the system under investigation, results for the relatively small molecule bithiophene, commonly used as a model for P3HT, were compared with those obtained using Møller−Plesset perturbation theory (MP2) and the substantial cc-pVDZ basis set,[32] which was assumed to produce proper energies. Various basis sets were tested and even the smallest basis sets captured the qualitative potential energy profile for torsion motion; the 3-21G* basis set was identified as an acceptable quantitative match while not overburdening the computational resources (results for other bases not shown). At all angles, the B3LYP/3-21G* method slightly underestimated the CTI when compared with MP2/cc-pVDZ results in the literature.

Unsubstituted bithiophene is often considered to be a reliable model for polythiophene and P3HT, with the exception of band gap calculations where the extended delocalization along multiple monomer units is critical. In this study, this hypothesis was examined by modeling regioregular alkyl-substituted oligothiophenes containing two, four, eight, and 14 units. Geometries were optimized to planar backbones for all oligomer lengths, which may not generally represent the global minimum of the potential energy hyperspace but do reflect the geometry of maximum mobility *and* that of experimental crystal structures,[26] and then the central inter-ring dihedral angle of the backbone was manually rotated in increments of 10° to model static torsional disorder. Single point energy calculations and population analyses were carried out at each angle. Both electronic structure and molecular orbital energies were explored to determine the minimal acceptable molecular model that captured the essential behavior of the polymer. Although the CTI provides an approximate quantitative measure of electronic coupling, and hence mobility, along polymer chains, a quick qualitative perspective can be obtained from examining the electronic structure of the frontier molecular orbitals. Figure 2 depicts HOMO and LUMO isodensity surfaces at various torsion angles for a chain consisting of eight monomers. Results are similar to those for all chain lengths that were studied.

Despite the common belief that breaking the planarity of the thiophene backbone destroys the conjugation, these orbitals remain essentially evenly distributed along the full complement of rings in the oligomer regardless of the torsion angle. This result is somewhat unintuitive because it is the out-of-plane p_z orbitals of the ring atoms that participate in the conjugated states, and these orbitals become increasingly orthogonal as the inter-ring dihedral angle is rotated away from the optimized planar geometry. For the extreme case of 90° torsion, the MOs presented in Figure 2 are localized on one-half of the molecule; however, for both the HOMO and the LUMO, these orbitals are in effect degenerate with the HOMO−1 and LUMO+1 MOs, respectively, as will be shown later in Figure 3. The localization of the latter MOs is on the complementary half of the molecule. Degeneracy of these orbitals implies that electrons (or holes) populating, e.g., the HOMO are free to cross through the rotated torsion angle to the HOMO−1-though symmetry issues may arise. From this simplistic picture, it appears that torsional defects play a less significant role in inhibiting mobility than generally thought.

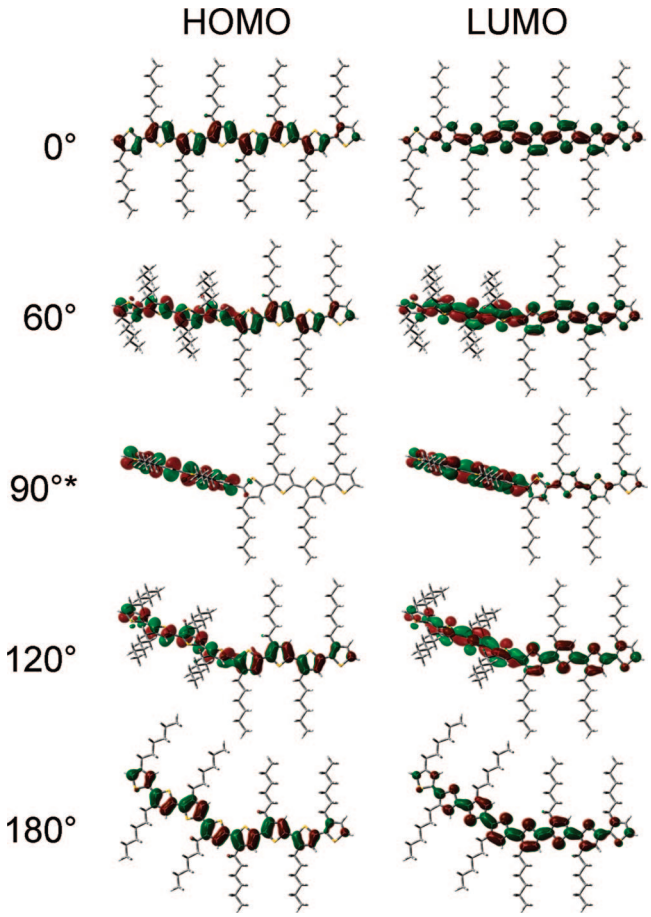

Figure 2. HOMO and LUMO isodensity surfaces for various rotations around the central backbone dihedral angle in $(P3HT)_8$. For all geometries studied between 0° and 180° (10° increments), the electron density is delocalized along the full length of the molecule. *HOMO and LUMO at 90° torsion are both nearly degenerate (Figure 3) with MOs having electronic structure localized on the other half of the oligomer backbone.

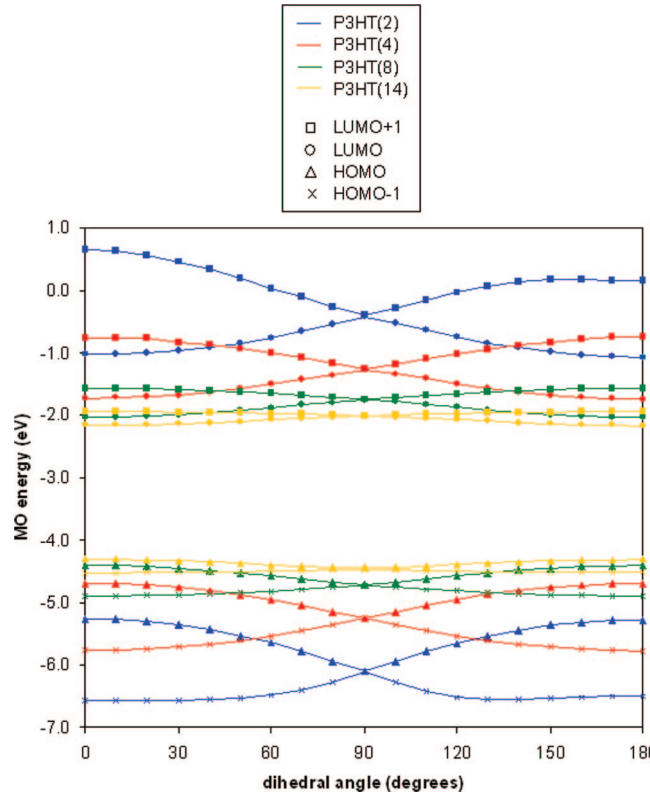

Figure 3. Frontier molecular orbital energies for various oligomers of P3HT as a function of the central inter-ring dihedral angle. Different oligomers are represented by different colors, and the MO designations are represented by the shape of the markers.

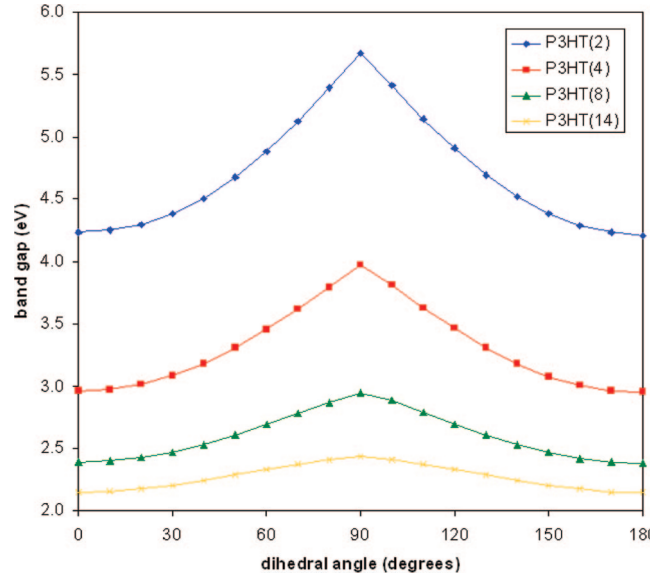

Figure 4. Calculated band gaps (HOMO−LUMO energy differences) for various oligomers of P3HT as a function of the central inter-ring torsion angle.

A more rigorous analysis involves application of eq 1 to the systems under examination. Molecular orbital energies for each oligomer are depicted in Figure 3.

Though the energy scales vary with oligomer length, the behavior is similar for each of the molecules, namely, as the torsion angle progresses from planar to 90°, the HOMO−1 and LUMO gradually increase in energy whereas the HOMO and LUMO+1 are stabilized. This trend is reversed on the other side of 90°, with the exception of $(P3HT)_2$ in which the HOMO−1 and LUMO+1 orbitals display a destabilizing and stabilizing trend, respectively, in the range 130°−180°. For each case, the result of the energy drift is that both the HOMO and HOMO−1 orbitals and the LUMO and LUMO+1 orbitals become nearly degenerate at 90°. These data provide a reasonable estimate of the optical band gap, i.e., the energy difference between the HOMO and LUMO, which is shown in Figure 4 for each of the oligomers.

Depending on the length of the oligomer, the band gap varies from 0.3 eV for $(P3HT)_{14}$ to as much as 1.5 eV for $(P3HT)_2$ as the torsion angle is rotated. These results have interesting potential ramifications for polymer-based optoelectronic devices. Because the variance decreases as the number of monomer units increases, for very long polymer chains the effect will be minimal. However, using the existing trend in the data to extrapolate the gap variance out to longer systems suggests that for oligomers of $n \leq 30$ torsional defects will play a significant (>100 meV) role in the optical absorption profile. Experimental values for the optical gap in P3HT are typically in the range of 2.0−2.2 eV;[40] though real systems are likely composed of an ensemble of active chain lengths, the 14-mer molecule calculated here has a good agreement with this average behavior. In photovoltaic devices, the active material absorbs most efficiently at the wavelength of its optical gap. Longer wavelength photons do not have sufficient energy to create excitons and shorter wavelength photons lose their extra energy to waste heat.

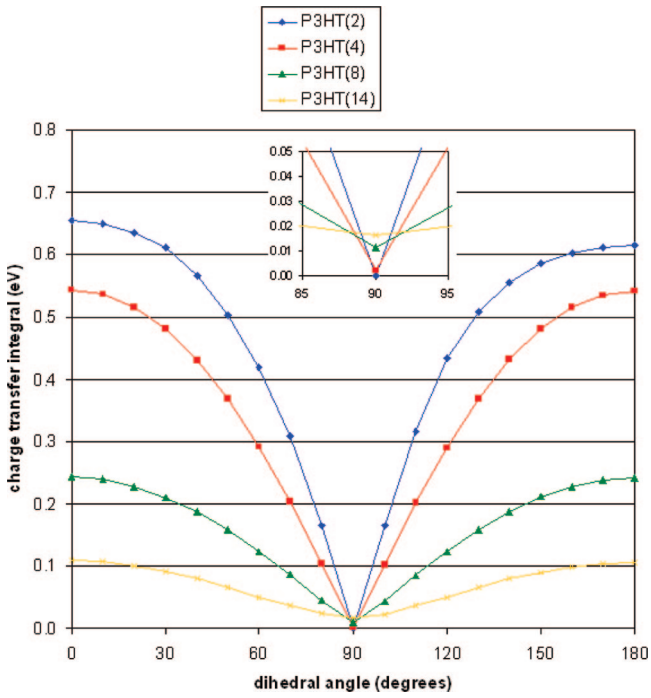

Figure 5. Calculated charge transfer integral for various oligomers of P3HT as a function of the central inter-ring torsion angle. This value provides an approximate quantitative measure of the electronic coupling between neighboring units. The inset represents the region close to 90°, showing that the coupling is nonzero and increases with the oligomer length.

Therefore, an active material containing components with a range of optical gaps could, in principle, be more efficient at converting light energy to electrical energy, which is to say that some of the reported loss in mobility associated with torsional defects may be mitigated by an expanded absorption envelope.

Using the orbital energies presented in Figure 3 along with corresponding calculations for moieties representing the separated halves of each molecule, it is possible to calculate the CTI as a function of inter-ring dihedral angle rotation. The results from this procedure are presented in Figure 5.

Applying the set of approximations raveled together in eq 1 to oligomers of $n > 2$ requires the additional approximation that each planar half of the molecule, composed of multiple rings, can be treated as a unit. There are surely some limitations to this approach, such as the fact that the calculated CTI for 0° torsion decreases significantly with increasing chain length, but this assumption is reasonable for deciphering trends given the extended conjugation present in the planar structures. A key observation from Figure 5 is that the CTI at 90°, which is expected to be essentially zero on the basis of bithiophene models, has a finite value that increases with oligomer length. One concludes, therefore, that the bithiophene model overestimates the torsion-induced mobility decrease in P3HT. Inclusion of the alkyl side chains in the calculations significantly increases the computational demands and likely has minimal effect on the electronic structure. From Figure 2 it is clear that the side chains play virtually no role in the frontier MOs. However, these chains play crucial roles in the torsional energy profiles. This effect is currently under study.[41]

Intramolecular mobility and band gap are both key parameters that determine device performance in polymer electronics and optoelectronics. Although it is known that structural defects are responsible for drastic variation in device operation, little is known about the relative roles of specific geometric defects. DFT calculations have indicated that minimal models for P3HT, though valuable in predicting some behavior, do not fully capture the effects of static inter-ring torsion defects. Explicit inclusion of additional monomer units and side chains provides additional insight. It reveals a surprising delocalization of frontier molecular orbitals through the nonplanar bonding configuration and band gap drift that may help to lessen the impact of torsion defects on charge carrier mobility in some devices. This work and further extensions to other types of molecular defects may guide processing methods[42] by highlighting which particular defects govern the intrinsic parameters of interest.

Acknowledgment. The author thanks M. Sternberg, J. Guest, and J. Greeley for useful discussions. Use of the Center for Nanoscale Materials was supported by the U.S. Department of Energy, Office of Science, Office of Basic Energy Sciences, under Contract No. DE-AC02-06CH11357.

References and Notes

(1) Zaumseil, J.; Sirringhaus, H. *Chem. Rev.* **2007**, *107*, 1296.
(2) Gunes, S.; Neugebauer, H.; Sariciftci, N. S. *Chem. Rev.* **2007**, *107*, 1324.
(3) Facchetti, A.; Yoon, M.-H.; Stern, C. L.; Hutchison, G. R.; Ratner, M. A.; Marks, T. J. *J. Am. Chem. Soc.* **2004**, *126*, 13480.
(4) Facchetti, A.; Mushrush, M.; Yoon, M. H.; Hutchison, G. R.; Ratner, M. A.; Marks, T. J. *J. Am. Chem. Soc.* **2004**, *126*, 13859.
(5) *Organic Photovoltaics: Mechanisms, Materials, and Devices*; Sun, S.-S., Sariciftci, N. S., Eds.; Taylor & Francis: New York, 2005; Vol. 99.
(6) Fichou, D. *J. Mater. Chem.* **2000**, *10*, 571.
(7) Northrup, J. E. *Phys. Rev. B* **2007**, *76*, 245202.
(8) Brinkmann, M.; Aldakov, D.; Chandezon, F. *Adv. Mater.* **2007**, *19*, 3819.
(9) Tsumura, A.; Koezuka, H.; Ando, T. *Appl. Phys. Lett.* **1986**, *49*, 1210.
(10) Bao, Z.; Dodabalapur, A.; Lovinger, A. J. *Appl. Phys. Lett.* **1996**, *69*, 4108.
(11) Sirringhaus, H.; Tessler, N.; Friend, R. H. *Science* **1998**, *280*, 1741.
(12) Cornil, J.; Brédas, J.-L.; Zaumseil, J.; Sirringhaus, H. *Adv. Mater.* **2007**, *19*, 1791.
(13) Horowitz, G.; Hajlaoui, M. E. *Adv. Mater.* **2000**, *12*, 1046.
(14) Zen, A.; Pflaum, J.; Hirschmann, S.; Zhuang, W.; Jaiser, F.; Asawapirom, U.; Rabe, J. P.; Scherf, U.; Neher, D. *Adv. Func. Mater.* **2004**, *14*, 757.
(15) Kline, R. J.; McGehee, M. D.; Kadnikova, E. N.; Liu, J.; Fréchet, J. M. J. *Adv. Mater.* **2003**, *15*, 1519.
(16) Goh, C.; Kline, R. J.; McGehee, M. D.; Kadnikova, E. N.; Fréchet, J. M. J. *Appl. Phys. Lett.* **2005**, *86*, 122110.
(17) Kumar, P.; Chand, S.; Dwivedi, S.; Kamalasanan, M. N. *Appl. Phys. Lett.* **2007**, *90*, 023501.
(18) Blom, P. W. M.; de Jong, M. J. M.; van Munster, M. G. *Phys. Rev. B* **1997**, *55*, R656.
(19) Ficker, J.; von Seggern, H.; Rost, H.; Fix, W.; Clemens, W.; McCulloch, I. *Appl. Phys. Lett.* **2004**, *85*, 1377.
(20) Coropceanu, V.; Cornil, J.; da Silva Filho, D. A.; Olivier, Y.; Silbey, R.; Brédas, J.-L. *Chem. Rev.* **2007**, *107*, 926.
(21) Sirringhaus, H. *Adv. Mater.* **2005**, *17*, 2411.
(22) Heeger, A. J.; Kivelson, S.; Schrieffer, J. R.; Su, W.-P. *Rev. Mod. Phys.* **1988**, *60*, 781.
(23) Osiele, O. M.; Britton, D. T.; Härting, M.; Sperr, P.; Topič, M.; Shaheen, S. E.; Branz, H. M. *J. Non-Cryst. Solids* **2004**, *338*−*340*, 612.
(24) Goris, L.; Poruba, A.; Purkrt, A.; Vandewal, K.; Swinnen, A.; Haeldermans, I.; Haenen, K.; Manca, J. V.; Vaněček, M. *J. Non-Cryst. Solids* **2006**, *352*, 1656.
(25) Nishiyama, F.; Ogawa, K.; Tanaka, S.; Yokoyama, T. *J. Phys. Chem. B* **2008**, *112*, 5272.
(26) Chen, T.-A.; Wu, X.; Rieke, R. D. *J. Am. Chem. Soc.* **1995**, *117*, 233.
(27) Salzner, U.; Lagowski, J. B.; Pickup, P. G.; Poirier, R. A. *J. Comput. Chem.* **1997**, *18*, 1943.
(28) Jones, D.; Guerra, M.; Favaretto, L.; Modelli, A.; Fabrizio, M.; Distefano, G. *J. Phys. Chem.* **1990**, *94*, 5761.
(29) Telesca, R.; Bolink, H.; Yunoki, S.; Hadziioannou, G.; van Duijnen, P. T.; Snijders, J. G.; Jonkman, H. T.; Sawatzky, G. A. *Phys. Rev. B* **2001**, *63*, 155112.
(30) Alguno, A. C.; Chung, W. C.; Bantaculo, R. V.; Vequizo, R. M.; Miyata, H.; Ignacio, E. W.; Bacala, A. M. *NECTEC Tech. J.* **2001**, *2*, 215.

(31) Yu, Z. G.; Smith, D. L.; Saxena, A.; Martin, R. L.; Bishop, A. R. *Phys. Rev. Lett.* **2000**, *84*, 721.

(32) Grozema, F. C.; van Duijnen, P. T.; Berlin, Y. A.; Ratner, M. A.; Siebbeles, L. D. A. *J. Phys. Chem. B* **2002**, *106*, 7791.

(33) van Eijck, L.; Johnson, M. R.; Kearley, G. J. *J. Phys. Chem. A* **2003**, *107*, 8980.

(34) van Eijck, L.; Senthilkumar, K.; Siebbeles, L. D. A.; Kearley, G. J. *Physica B* **2004**, *350*, 220.

(35) da Silva Filho, D. A.; Coropceanu, V.; Fichou, D.; Gruhn, N. E.; Bill, T. G.; Gierschner, J.; Cornil, J.; Brédas, J.-L. *Phil. Trans. R. Soc. A* **2007**, *365*, 1435.

(36) Viruela, P. M.; Viruela, R.; Orti, E. *Int. J. Quantum Chem.* **1998**, *70*, 303.

(37) e Silva, G. M.; de Brito, A. N.; Correia, N. *Phys. Rev. B* **1996**, *53*, 7222.

(38) Vekhter, B. G.; Ratner, M. A. *J. Chem. Phys.* **1994**, *101*, 9710.

(39) Frisch, M. J.; Trucks, G. W.; Schlegel, H. B.; Scuseria, G. E.; Robb, M. A.; Cheeseman, J. R.; Montgomery, J. A., Jr.; Vreven, T.; Kudin, K. N.; Burant, J. C.; Millam, J. M.; Iyengar, S. S.; Tomasi, J.; Barone, V.; Mennucci, B.; Cossi, M.; Scalmani, G.; Rega, N.; Petersson, G. A.; Nakatsuji, H.; Hada, M.; Ehara, M.; Toyota, K.; Fukuda, R.; Hasegawa, J.; Ishida, M.; Nakajima, T.; Honda, Y.; Kitao, O.; Nakai, H.; Klene, M.; Li, X.; Knox, J. E.; Hratchian, H. P.; Cross, J. B.; Bakken, V.; Adamo, C., Jaramillo, J.; Gomperts, R.; Stratmann, R. E.; Yazyev, O.; Austin, A. J.; Cammi, R.; Pomelli, C.; Ochterski, J. W.; Ayala, P. Y.; Morokuma, K.; Voth, G. A.; Salvador, P.; Dannenberg, J. J.; Zakrzewski, V. G.; Dapprich, S.; Daniels, A. D.; Strain, M. C.; Farkas, O.; Malick, D. K.; Rabuck, A. D.; Raghavachari, K.; Foresman, J. B.; Ortiz, J. V.; Cui, Q.; Baboul, A. G.; Clifford, S.; Cioslowski, J.; Stefanov, B. B.; Liu, G.; Liashenko, A.; Piskorz, P.; Komaromi, I.; Martin, R. L.; Fox, D. J.; Keith, T.; Al-Laham, M. A.; Peng, C. Y.; Nanayakkara, A.; Challacombe, M.; Gill, P. M. W.; Johnson, B.; Chen, W.; Wong, M. W.; Gonzalez, C.; Pople, J. A. *Gaussian 03*, revision D.01; Gaussian, Inc.: Wallingford, CT, 2004.

(40) Koster, L. J. A.; Mihailetchi, V. D.; Blom, P. W. M. *Appl. Phys. Lett.* **2006**, *88*, 093511.

(41) Darling, S. B.; Sternberg, M. Submitted for publication.

(42) Darling, S. B. *Prog. Polym. Sci.* **2007**, *32*, 1152.

JP8017919